Purdue University
Purdue e-Pubs

Department of Computer Science Technical Reports | Department of Computer Science

1992

Two Dimensional MAT to Boundary Conversion

Pamela J. Vermeer

Report Number:

92-071

TWO-DIMENSIONAL MAT TO BOUNDARY CONVERSION

Pamela J. Vermeer

CSD-TR-92-071
September 1992

Two-dimensional MAT to Boundary Conversion

Pamela J. Vermeer
Purdue University

September 22, 1992

Abstract

The medial axis transform (MAT) has potential as a powerful representation for a conceptual design tool for objects with inherent symmetry or near-symmetry. The medial axis of two-dimensional objects or medial surface of three-dimensional objects provides a conceptual design base, with transition to a detailed design occuring when the radius function is added to the medial axis or surface, since this additional information completely specifies a particular object. To make such a design tool practicable, however, it is essential to be able to convert from an MAT format to a boundary representation of an object. Such a conversion is possible because the MAT is an informationally complete solid representation.

In this paper, we provide the details for the conversion of the MAT of a set of two-dimensional objects to a boundary representation. We demonstrate certain smoothness properties of the MAT and show the relationship between the tangent to the MAT at a point and the boundary points related to that MAT point. For each of the three general types of MAT points (end points, normal points, and branch points) we detail the method for obtaining the boundary points related to it and for determining whether finite contact occurs at that point. We discuss requirements for an MAT to be valid in the sense that the given curves could actually be the MAT of an allowable two-dimensional object. We also provide a theoretical error bound on the computation. Finally, we discuss an implementation of our algorithm and show some results we have obtained.

1 Introduction

The medial axis transform (MAT) has potential as an alternative representation for certain design and modeling problems [HV92]. To exploit this potential, however, it is essential that the boundary of the object which an MAT represents be easily determined. For two-dimensional objects, the MAT consists of curves in three-space. Given a valid MAT, that is, a set of curves which comprise the MAT of a valid boundary as defined below, the boundary points related to any particular point on the MAT can be found, based solely on the MAT point and the tangent(s) to the MAT at the point. In this work, we demonstrate the relationship between the MAT tangent and the boundary points which forms the basis of this conversion. We also show a smoothness property of the MAT, and detail the requirements for a graph in three-space to be a valid MAT. We provide an error bound which shows how errors in a computed MAT relate to errors in the generated boundary. Finally we discuss our implementation of the conversion algorithm and show some examples.

2 Medial Axis Definitions and Properties

2.1 Restriction on Objects

In our theoretical development, we require that objects under consideration be simple, in the precise sense defined here:

Definition 2.1 *A 2D object O is simple if the following are satisfied:*

1. *O has an interior with finite area.*
2. *The interior of O is path-connected.*
3. *O has a finite number of boundary loops, all of which are simply connected closed curves with continuous tangent and curvature at all but a finite number of points. At points where the tangent or curvature does not exist, sided tangents and curvatures must exist.*

This definition is not overly restrictive, since most objects of interest in design situations satisfy these requirements inherently. Simple objects may have a finite number of interior voids, so that although the MAT will be connected, it need not be simply connected. Further, since each boundary loop is piecewise curvature continuous, the boundary curves are all locally parameterizable except possibly at points of connection between segments.

2.2 Definitions of the MAT

There are many definitions of the MAT, but for the current problem, two are particularly useful. The first of these is from Blum [Blu64], and depends on the notion of *maximal inscribed discs*, discs which are completely contained inside an object and which are contained in no other such disc. The *medial axis* (MA) or *skeleton* of an object is the closure of the locus of the centers of all maximal inscribed discs. For two-dimensional objects, the *medial axis transform* (MAT) is the set of space curves consisting of points (x, y, r) where (x, y) is an MA point specifying the location of the center of a maximal inscribed disc and r is the disc's radius. On the left in Figure 1 is a simple object and its MA, along with some of the maximal discs. On the right, the space curves comprising the MAT corresponding to the object is shown.

This definition provides a natural way to distinguish between types of MA points. The distinction is based on the number of touchings the disc centered at the point has with the boundary. A disc can touch with *point contact*, that is, a single boundary point touches a single point on the disc boundary, or with *finite contact*, in which a contiguous arc of points on the disc touches a segment of the boundary. Either type is considered a single touching.

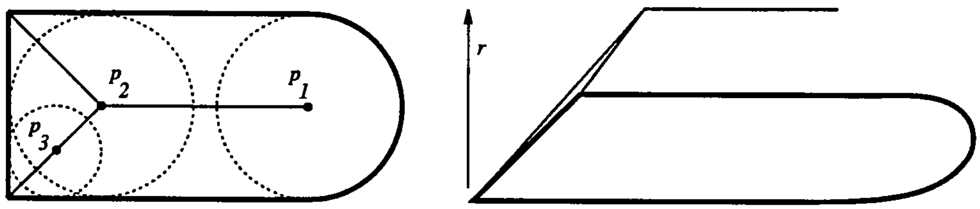

FIGURE 1: Some maximal inscribed circles and the MAT of a simple object

The *order* of a point is the number of touchings that the disc related to an MA point has with the boundary. An MA point of order one is an *end point*. *Normal points* are MA points of order two, and *branch points* are points with three or more boundary touchings. In Figure 1, p_1 is an end point, p_2 is a branch point, and p_3 is a normal point.

An alternative definition which provides insight into the geometric relationships between an object and its MAT is given in terms of *cyclographic maps* [HV92, Hof92, MK29]. Starting with a curve C in the xy-plane, a ruled surface is formed by the set of all lines through the curve which make a 45° angle with the xy-plane, increasing towards the interior of C, and whose projection onto the xy-plane is the normal to the curve at the intersection point of the curve and the line. Because the lines make a fixed angle with the plane, the surface is developable [MK29].

For a given point (x, y) in the plane, there may be multiple values of z such that (x, y, z) lies on the surface. If (x, y) is in the interior of C, take the point with positive z-value nearest to the xy-plane, and if it is exterior to C, take the point with negative z-value nearest to the xy-plane. The surface S so generated is single-valued and defined over the xy-plane, and the absolute value of the z-coordinate of each point on this surface gives the distance from (x, y) to C. The surface S has singularities at the points where two or more generating lines meet. The curves given by the closure of these singularities comprise the MAT. For a more complete discussion of the cyclographic map, see [HV92, Hof92].

2.3 MAT Properties

In the literature on the MAT and its applications, many properties have been suggested which are intuitively sensible, but formal proofs of these properties are generally lacking. Recent works by Chiang [Chi92] and Wolter [Wol92] have filled in some of these gaps. We mention some relevant results of theirs, and we state and prove a smoothness property of the MAT here.

One important property of the MAT is its uniqueness. That is, given any boundary there is exactly one MAT related to it, and given any MAT, there is exactly one boundary from which it could have been derived [Chi92]. Duda and Hart show informally and Wolter has shown rigorously that the boundary and interior of a simple object can be retrieved from the MAT by taking the union of all the maximal discs defined by the MAT [DH73, Wol92].

In the same paper, Wolter shows that the MA of a planar object whose boundary is a piecewise C^2 manifold has the same homotopy type as the boundary. Thus for simple objects as defined by Definition 2.1, the MA will be connected and have the same number of loops as the object has interior voids.

A final result from Wolter's work is that the MA is nowhere dense in $\Re^2$, which means that the MA of a planar object is a planar graph. These results have also been noted elsewhere, for example, [BN78, Gur89, PG90], but with no proofs provided.

Another property asserted by Blum and Nagel [BN78] but not proved is that the MAT of a simple object is differentiable at all but a finite number of points. In the following theorem we show that in fact the tangent is continuous everywhere but at a finite number of points.

Theorem 2.1 *The MAT of a simple object has a continuous tangent everywhere except at end points, branch points, and normal points of finite contact. At the exceptional points, a one-sided tangent exists from each approach to the point along the MAT.*

Proof: Let O be a simple object with boundary B, and let S be the positive portion of the cyclographic map of B. Since O is simple, for each boundary curve comprising B the surface element of S generated by that curve has a continuous tangent plane everywhere but at self-intersections. Thus S in its entirety has a continuous tangent plane everywhere but at self-intersections. Note that the self-intersections in S can occur either because a single surface element has self-intersections or because two or more surface elements intersect. The curves in the self-intersections of S arise from two surface sheets meeting tangentially, such as along an edge of regression, or from two surface sheets meeting transversally.

By definition, the MAT M corresponding to O consists of a subset of the self-intersection points of S along with the limit points of that subset. Because O is simple, M is connected, therefore there are no isolated MAT points. That is, the MAT is either a single point in the case of O being a disc, or it is a connected collection of curves. We claim that the only candidates for points on the MAT are the curves which come from a transverse intersection of two surface sheets and their limit points.

Consider a point $p = (x_0, y_0, z_0)$ on S with tangent plane T_p. Because T_p makes a 45° degree angle with the xy-plane, there is exactly one point b on the line obtained by intersecting T_p with the xy-plane which is distance z_0 from the projection of p to the xy-plane. Since the z-coordinate of a point on the cyclographic map must measure precisely this distance, the line bp is the only generating line to lie in T_p. Thus the number of tangent planes to S at p is exactly the same as the number of boundary points of O related to p. Therefore curves generated by two surface sheets meeting tangentially consist of points with only one related boundary point. By definition, such a point can be on the MAT if and only if it is a limit point of a set of points with two or more generating lines. Since O is simple, the MAT consists of only a finite number of curves, thus such limit points must be isolated. For if there were a curve segment of limit points, each point on it must be the limit point of a different transversal intersection curve, so there would be infinitely many such intersections.

Thus our claim holds. For the remaining curves, because the surface sheets which meet transversally are tangent plane continuous, the intersection curves must also be tangent continuous. From the previous paragraph, these points are exactly normal points with two related boundary points, since they have two tangent planes associated with them on S. The limit points of these curves are either end points or connections between tangent continuous components. The connection points could be finite contact normal points, where infinitely many tangent planes exist at the vertex of a conical surface element, or branch points, where three or more surface elements come together, including possibly branch points with finite contact. Since the curves are tangent continuous, a one-sided tangent exists from each approach to an end or connection point. □

Two important results are immediately obvious from the theorem.

Corollary 2.1 *Any point at which the MAT has a continuous tangent has exactly two related boundary points.*

Corollary 2.2 *End points, branch points, and normal points of finite contact are isolated on the MAT. That is, given an end point, branch point, or normal point of finite contact p, there is some ε such that any MAT point in an ε neighbohood of p is a normal point with only point contact with the boundary.*

3 Conversion Theory

The technique used for converting from the MAT to the boundary relies on insights about the MAT derived from the cyclographic map definition. The MAT tangent is the essential component of the method, and understanding how it is related to the boundary is the basis for the actual conversion. We begin by detailing this relationship. Subsequently, we demonstrate how to locate all of the related boundary points for each type of MAT point using the MAT tangent.

Throughout this section we rely on the assumption that each curve of the MAT is parameterized with respect to arclength. We will also without further notice use the notation that $\overline{p} = (\overline{x}, \overline{y}, \overline{r})$ is a point on the MAT M of a simple object O and that p is its projection to the MA S. The MAT tangent at $\overline{p}$ is referred to as T_M while the tangent to S at p is given by T_S. Note that T_S is the projection of T_M to the xy-plane.

3.1 Fundamental Underpinnings

The three lemmas in this section demonstrate the basic relationship between the MAT tangent and the related boundary.

Lemma 3.1 *Let $\overline{p}$ be an MAT point with a continuous tangent and whose related boundary points each have a unique normal. Let q_1 and q_2 be the points on the boundary related to $\overline{p}$. Then T_S bisects the angle between the normals to q_1 and q_2.*

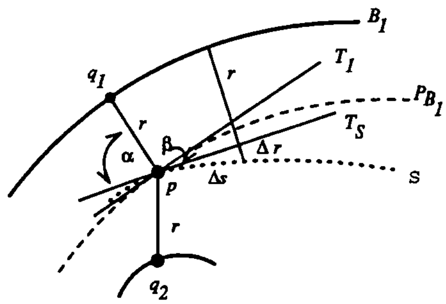

FIGURE 2: Relationship between MA tangent and boundary tangent

Proof:

The proof is based on Figure 2, from Blum [Blu73]. Here p is a point of the MA S (shown as a dotted line) distance r from the boundaries. B_1 is one side of the boundary, and P_{B_1} is the parallel curve to B_1 offset a distance r. Let β be the angle between the tangent T_1 to the boundary parallel and the MA tangent T_S, while α is the angle between the boundary normal and the MA tangent. Consider the derivative dr/ds:

$$\begin{aligned} \frac{dr}{ds} &= \lim_{\Delta s \to 0} \frac{r(s+\Delta s) - r(s)}{\Delta s} \\ &= \lim_{\Delta s \to 0} \frac{\Delta r}{\Delta s} \\ &= \sin \beta \end{aligned}$$

since in the limit, the arc indicated by Δs is the tangent to the MA, and the arc along the boundary parallel is the tangent to the boundary parallel at p. By a simple transformation,

$$\cos \alpha = \frac{dr}{ds}$$

Since the boundary side was chosen arbitrarily, this angle is the same for both boundaries, and hence the MA tangent bisects the angle between the two normals. □

In the next lemma, we show the relationship between the tangent to the MAT, the MA tangent and the boundary tangents at the related boundary points. Müller provides a different proof of this relationship in the context of cyclographic maps [MK29].

Lemma 3.2 *Let $\overline{p} = (x(s_0), y(s_0), r(s_0))$ be a point at which M has a continuous tangent and whose related boundary points q_1 and q_2 each have a unique normal. Then T_1, T_2, and T_M are concurrent along T_S, where T_i is the tangent to the boundary at q_i.*

Proof:

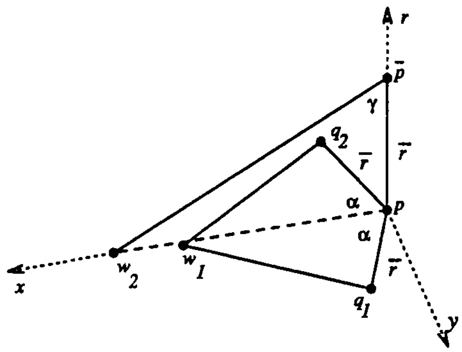

FIGURE 3: Triangles relating boundary, MAT, and MA tangents

By Lemma 3.1, if T_1 and T_2 intersect T_S they do so at a single point w_1, as shown in Figure 3. Also, since T_S is the projection of T_M into the xy-plane, T_M must intersect T_S at the point w_2 on T_M with r-coordinate 0. We show that w_1 and w_2 are equal distance from p.

Consider the two triangles in the xy-plane in Figure 3. Let l_1 be the length of the segment from p to w_1. The angle $\angle p\, q_1\, w_1$ is a right angle since $\overline{p\, q_1}$ is the boundary normal at p_1 and $\overline{q_1 w_1}$ is the boundary tangent at q_1. Thus

$$l_1 = \frac{\bar{r}}{\cos\alpha}$$

where $\bar{r} = r(s_0)$.

Now consider the triangle $\bar{p}\, p\, w_2$. For ease of notation, we will assume that all derivatives are evaluated at s_0. Without loss of generality, assume that $\bar{p} = (0, 0, \bar{r})$ and that $y' = 0$, and consider the problem in the xr-plane. Let l_2 be the length of the segment from p to w_2, so that w_2 has coordinates $(l_2, 0)$. Then the direction vector along the hypotenuse of the triangle is

$$(x', r')/L$$

where

$$L = \sqrt{x'^2 + r'^2}$$

Since the direction vector of the leg with length $\bar{r}$ is (0, 1),

$$\cos\gamma = \frac{\bar{r}}{\sqrt{(l_2^2 + \bar{r}^2)}} = (0,1)\cdot(x', r') = \frac{r'}{L}$$

where $\gamma = \angle\bar{p}\, p\, w_2$. Solving for l_2, we obtain

$$l_2 = \frac{\bar{r}}{r'}x'$$

But since the segment has an arc length parameterization and $y' = 0$, $x' = 1$. Also, we know from the proof of Lemma 3.1 that $r' = \cos\alpha$. Thus

$$l_2 = \frac{\overline{r}}{\cos\alpha}$$

which is the same as l_1. Thus if T_1 and T_2 intersect, then $w_1 \equiv w_2$.

If T_1 and T_2 do not intersect, then $\alpha = \pi/2$, so that $\cos\gamma = 0$ and T_M must be parallel to the xy-plane. In this case, all four lines are parallel and thus have in common a point at infinity, so the lemma holds. □

Both Lemma 3.1 and 3.2 depend on the existence of a unique normal at each boundary point related to $\overline{p}$. However, these results hold even when there is no unique boundary normal, such as when two boundary components meet in a concave corner.

Lemma 3.3 *Let $\overline{p}$ be a point at which M has a continuous tangent. Let q_1 and q_2 be the two boundary points related to $\overline{p}$. Then Lemmas 3.1 and 3.2 hold if the normals to the boundary B at q_1 and q_2 are replaced with the connecting lines $\overline{p\,q_1}$ and $\overline{p\,q_2}$, respectively.*

Proof:

Let l_1 and l_2 be the line segments connecting q_1 and q_2 to p, respectively, and let T_1 and T_2 be the normals to these line segments. Notice that if B has a unique tangent at q_1, then l_1 is the normal to B at q_1, and T_1 the tangent there, and similarly for q_2.

Referring to Figure 2, the calculation of dr/ds in the proof of Lemma 3.1 followed because in the limit, a right triangle was determined by the boundary parallel tangent, the boundary normal, and the MA tangent. Since we have chosen T_1 to be normal to l_1, as we move along the MA towards p, we have the same relationship in the limit, namely,

$$\frac{dr}{ds} = \sin\beta$$

As before, since the radial line chosen was arbitrary, this relationship must hold for either the angle between T_S and l_1 or between T_S and l_2, thus the angles must be identical.

Lemma 3.2 depends on the existence of the boundary normals only to apply Lemma 3.1, and thus the proof of this follows immediately. □

From Theorem 2.1, when there is a discontinuity in the MAT tangent there are no longer exactly two related boundary points. We will discuss the various possibilities for the boundary in the following sections where we give the details of locating the related boundary points for each type of MAT point.

3.2 MAT to Boundary Conversion

Using Theorem 2.1 and Lemmas 3.1, 3.2, and 3.3, we can classify the boundary points related to the various types of MA points. We start by considering normal points, which can be further subdivided into two categories. First we locate boundary points for normal points which have a continuous tangent, whether or not the related boundary points also have a continuous tangent. Then we consider the situation where the tangent to the MA at a normal point has a discontinuity. Next we demonstrate how to find the boundary points related to end points, and finally, we show how to determine those related to branch points.

3.2.1 Smooth normal points

The basic technique for finding boundary points related to an MAT point $\overline{p}$ is to find the angle which the radial line connecting p to a related boundary point makes with the MA tangent at p. Related boundary points then must lie along those lines, distance $\overline{r}$ from p. For normal points at which the MAT tangent is continuous, the two related boundary points can be found by directly applying Lemma 3.3. For completeness sake, we demonstrate how to do this here; the method is also described in [HV92]. For other types of MAT points, this technique can be applied in a modified form to find all related boundary points.

Theorem 3.1 *Let $\overline{p}$ be a normal point with a continuous tangent on M. Then the boundary points q_1 and q_2 associated with $\overline{p}$ can be determined exactly from the tangent T_M to M at $\overline{p}$.*

Proof:

In Figure 4, let l_1 and l_2 be the line segments connecting p to q_1 and q_2, respectively, and let T_1 be perpendicular to l_1 at q_1, and T_2 be perpendicular to l_2 at q_2. Then from the proof of Lemma 3.3 the angles β_1 and β_2 between the MA tangent and the lines T_1 and T_2 are well-defined and equal. Thus the angle α between T_S and either radial line l_1 or l_2 is well-defined.

From Lemma 3.2, the angle can be computed as

$$\alpha = \arccos \frac{\overline{r}}{l}$$

where l is the length of the line segment from p to w, the intersection of the tangent with the xy-plane. This computation of α forces the restriction that $0 \leq \alpha \leq \pi/2$. This simply means that in the xy-plane, the angle α must be measured from the ray of T_S pointing

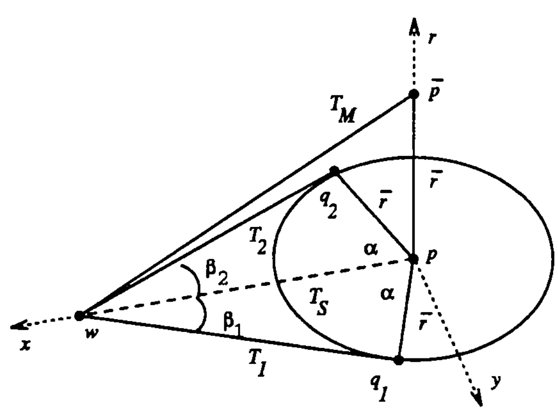

FIGURE 4: α is uniquely determined by $\overline{r}$ and l

in the direction of decreasing r. The boundary points q_1 and q_2 can then be found by a rotation about p of a line segment with length $\overline{r}$.□

3.2.2 Finite contact normal points

As long as a normal point has continuous derivatives, there are exactly two boundary points related to it. However, when a discontinuity occurs in either the MA or the radius function at a normal point, finite contact occurs on at least one of the boundary touchings. By extending Theorem 3.1 to points on the MAT with a one-sided tangent, we can determine all of the boundary points related to such a point, whether the contact is finite or discrete.

Lemma 3.4 *Suppose $p_0 = (x(s_0), y(s_0), r(s_0))$ is an MAT point at which the tangent has a discontinuity. Let S_i be a tangent-continuous approach to p_0 along M, and let $T_i = (x'(s_i), y'(s_i), r'(s_i))$ be the tangent at any point s_i on S_i. Let*

$$T_0 = \lim_{s_i \to s} T_i$$

and

$$\alpha_0 = \lim_{s_i \to s} \alpha_i$$

where α_i is the angle between T_i and either radial line to the boundary points related to $p_i = (x(s_i), y(s_i), r(s_i))$, computed as in Theorem 3.1. Then two boundary points q_1 and q_2 related to p_0 can be found as the points distance $r(s_0)$ from p_0 along the line segments emanating from p_0 at an angle α_0 to T_0, measured in the direction of decreasing r.

Proof:

This follows directly from the continuity of the angle α_i along S_i and the continuity of the boundary. □

Based on this lemma, we can immediately find the boundary points related to a normal point with a tangent discontinuity.

Theorem 3.2 *Let $\overline{p}$ be a normal point of the MAT M which has a discontinuity in the derivative of one of its component functions. Let S_1 and S_2 be the the two MA segments adjoining $\overline{p}$. Then the boundary points related to p can be found from the two one-sided tangents T_{M_1} and T_{M_2} to the MAT at p.*

Proof:

From Lemma 3.4, two points q_{11} and q_{12} on the boundary related to *op* can be found using the one-sided tangent T_{M_1} approaching *op* along S_1, and two more points q_{21} and q_{22} can be found using T_{M_2}. If a direction is chosen arbitrarily at *op*, each pair of points can be split into one point which lies on the left and one which lies on the right of the MAT at *op*. Suppose that q_{i1} lies on the left for $i = 1, 2$, and q_{i2} lies on the right. Consider the points on the left. Either they are identical, and so the disc related to *op* makes discrete contact with the boundary, or they are distinct. Since *op* is a normal point, it must have

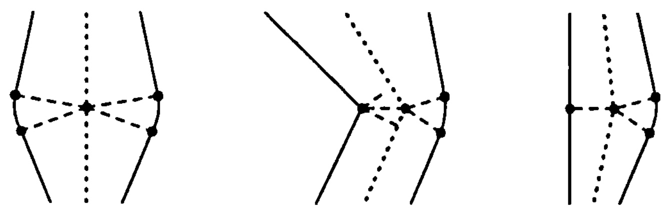

FIGURE 5: Finite contact can occur on one or both sides. (Adapted from Blum and Nagel)

exactly one touching with the boundary on either side of the MAT, thus q_{11} and q_{12} must delimit the arc of the disc which touches the boundary. This holds similarly on the right side of the MAT. □

While this theorem asserts that the boundary points can be found and demonstrates a way to find them, it gives no indication how to predetermine whether the touchings on one or both sides will be finite contact or discrete contact. As pointed out in [BN78], any combination is possible, see Figure 5, but no criteria are given for which situation holds. The situations which arise can be classified, however, based on the type of discontinuity in the MAT tangent. This classification is discussed in Section 4, in the context of locally valid connections of MAT segments.

3.2.3 End Points

There are three situations possible for end points, but all of them can be handled identically, by applying Lemma 3.4. Examples of the three situations are shown in Figure 6, where the end points and the boundary points related to each end point are highlighted. One possibility is that the end point is related to a convex corner in the boundary. This can be immediately discerned, since it is the only time that an MAT point can have its radius function equal to zero. A second possibility is that the end point is related to a single point, but $r \neq 0$. This occurs when the maximally inscribed circle is the same as the circle of curvature, as is the case with the end point of the MA of a parabola. The final possible situation is that the disc makes finite contact with the boundary. The following theorem demonstrates the computation of the boundary element for an end point.

Theorem 3.3 *Let M be the MAT of a planar object and let $\overline{p}$ be an end point of M. Then the boundary points associated with $\overline{p}$ can be determined from the one-sided tangent T_M at $\overline{p}$.*

Proof:

Let S be the segment of M adjacent to $\overline{p}$ and let T_M be the one-sided tangent to M at $\overline{p}$ approaching along S. Let $\overline{r}$ be the radius at $\overline{p}$ and l be the length of T_M between

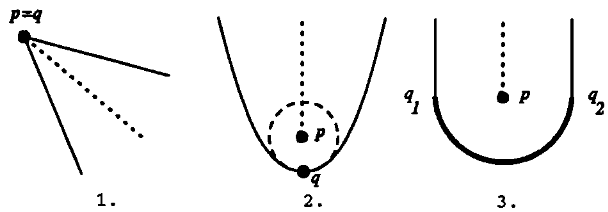

FIGURE 6: Three types of contact are possible for end points.

the projection p of $\overline{p}$ to the xy-plane and the intersection of T_M with the xy-plane. By Lemma 3.4, two boundary points related to $\overline{p}$ can be found by computing the angle

$$\alpha = \lim_{s \to s_i} \alpha_i = \lim_{s \to s_i} \arccos \frac{r_i}{l_i} = \arccos \frac{\overline{r}}{l}$$

where s_i is the parameter value of a point p_i on S, r_i is the radius component of p_i, and l_i is the length of the tangent projection line between p_i and w_i, as in Theorem 3.1.

If $\alpha = 0$ then no rotation occurs, so a single point is related to $\overline{p}$. Otherwise, two points q_1 and q_2 are found which are the points adjacent to the boundary components related to S. Since $\overline{p}$ is an end point, it can have only one touching with the boundary, and so the circular arc of radius r bounded by q_1 and q_2 and not intersecting S must be the boundary related to $\overline{p}$. □

3.2.4 Branch Points

The only points of the MAT yet to be considered are branch points. The boundary points related to a branch point can be found by applying Lemma 3.4.

Theorem 3.4 *Let M be an MAT of a planar object and let $\overline{p}$ be a branch point of order n. Let the branches of the MAT be given by S_i, $i = 0 \,..\, n-1$, with S_1 being chosen arbitrarily, and the subsequent S_i being listed in counterclockwise order about $\overline{p}$. Then the boundary points related to $\overline{p}$ can be found from the one-sided tangents T_{M_i}, $i = 0 \,..\, n-1$ to the MAT at $\overline{p}$.*

Proof

Throughout this proof, we assume mod n arithmetic for the subscripts, so that S_0 is the same as S_n. Consider any branch S_i and the one-sided tangent T_{M_i} obtained by approaching $\overline{p}$ along S_i. By Lemma 3.4, two boundary points q_{i1} and q_{i2} related to $\overline{p}$ can be found from T_{M_i}. Suppose that we have computed the related boundary points for $i = 0 \,..\, n-1$. Then between the projection of any two MAT branches S_i and S_{i+1} there are two such points. Order the points such that these two points are q_{i2} and $q_{(i+1)1}$. Since the order of the branch point is n, there must be exactly n touchings of the disc of radius r centered p with the boundary, one touching between any two branches. Hence, either q_{i2} is identical to $q_{(i+1)1}$, or q_{i2} and $q_{(i+1)1}$ delimit a circular arc of the disc between the two branches. □

Another way to conceptualize what occurs at a branch point is to consider it to be a multiple normal point. That is, for any two adjacent MAT branches compute the two related boundary components as though the branch point were a normal point. The boundary component between the MA branches is kept, while the other is discarded. By repeating this operation for each pair of adjacent branches, the related boundary points in each region are found.

4 Valid MATs

Based on the theory in Section 3, for any valid MAT we are able to determine the boundary related to it. However, for this to be useful, we need to be able to tell when a graph in three-space is the MAT of a valid object. It is clear that any planar graph has the potential to be the MA of some object. However, problems can arise when the radius dimension is included. Globally, the radius function may be too large at points, causing self-intersections of the boundary. This is difficult to detect without simply computing the boundary and checking it for self-intersections. Locally, the rate of change of the radius function is constrained by the relationship between the MAT tangent and the angle between the radial line and the MA tangent line. Also locally, tangent discontinuous connections between MA segments can give rise to invalid MATs if the radius function is not chosen carefully. In this section, we look at the requirements on the radius function, given the MA, to formulate a locally valid MAT.

At points with a unique tangent, the tangent must be such that the angle γ between T_M and the xy-plane is less than $\pi/4$. This restriction is necessary because

$$\tan\gamma = \cos\alpha = \frac{r}{l}$$

where l is the length of the line segment between the projection of $\overline{p}$ to the xy-plane and the point at which the tangent intersects the xy-plane. This relationship can be seen easily by considering Figure 4, where γ is the angle $\angle\,\overline{p}\,w\,p$. With respect to the tangent $(x'(s), y'(s), r'(s))$, satisfying this requires that

$$\frac{|r'(s)|}{\sqrt{(x'(s))^2 + (y'(s))^2}} \leq 1$$

At juncture points of the MAT, where there are multiple one-sided tangents, each tangent must satisfy the same requirement. Furthermore, only certain transitions are allowable between adjacent one-sided tangents. Recall from Theorem 2.1 that such points are either end points, branch points, or places where the maximal inscribed disc has finite contact with the boundary. The related boundary points are found by computing the boundary points using each tangent independently, and then connecting them by a circular arc if multiple points are found on any one side of the MA. This process is only valid, however, if the boundary points lie in proper positions relative to the given tangents. Theorem 4.1 explains the order required for validity for piecewise linear MATs. We restrict ourselves to this subset of MATs because the conversion algorithm we have implemented has as input a piecewise linear MAT. Since we know from Section 3.2.4 that branch points can be treated as multiple normal points, we will confine the present discussion to normal points and comment on the application to branch points when we present our algorithm.

Theorem 4.1 *Let $\overline{p}$ be a normal point of a piecewise linear MAT M, and suppose that at $\overline{p}$ M has two distinct one-sided tangents. Since M is piecewise linear, $\overline{p}$ is a juncture of two line segments, T_1 and T_2, and these are exactly the two tangents to M at $\overline{p}$. Let p be the projection of $\overline{p}$ to the xy-plane and let q_1 and q_2 be the projections of the other delimiters of T_1 and T_2, respectively. Let b_{11} and b_{12} be the two boundary points associated with $\overline{p}$ from T_1 and b_{21} and b_{22} those associated with $\overline{p}$ from T_2. If q_1, q_2, b_{11}, b_{12}, b_{21}, and b_{22} are circularly sorted around p, then for M to be valid it is necessary that the points are in one of the following orders:*

$$q_1\, b_{11}\, b_{21}\, q_2\, b_{22}\, b_{12}$$

$$q_1\, b_{12}\, b_{21}\, q_2\, b_{22}\, b_{11}$$

$$q_1\, b_{11}\, b_{22}\, q_2\, b_{21}\, b_{12}$$

$$q_1\, b_{12}\, b_{22}\, q_2\, b_{21}\, b_{11}$$

Proof:

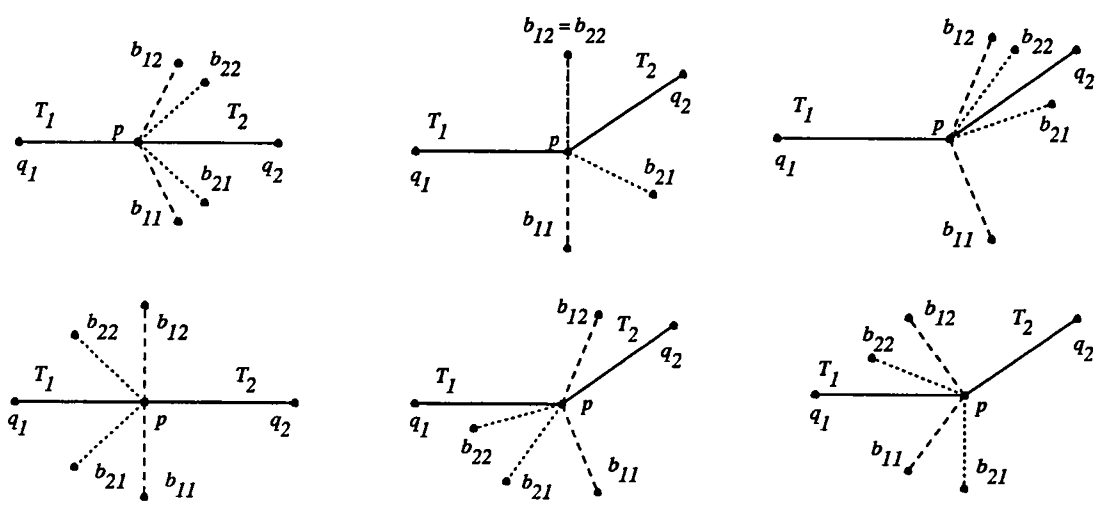

FIGURE 7: The top three situations are valid, while the bottom three are invalid.

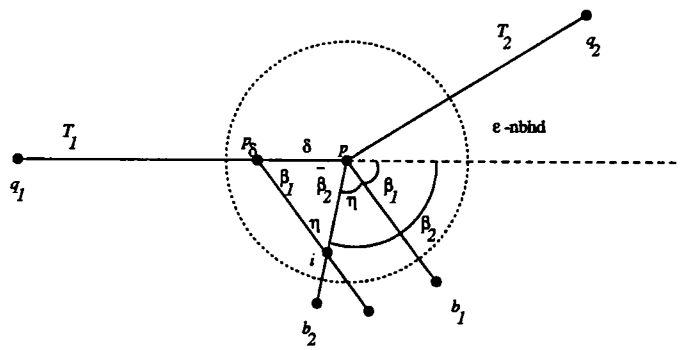

FIGURE 8: An illegal intersection occurs when the radial lines have invalid order

Figure 7 shows a visual interpretation of this theorem, where the upper figures are valid while the lower figures are invalid. We will show that this ordering is necessary by showing that if a boundary point from T_2 is radially nearer to q_1 than a boundary point from T_1, then a nearby generating line along T_1 intersects the generating line from T_2, thereby producing an extraneous MAT point. Specifically, since $\overline{p}$ is a normal point, there exists some ε such that in an ε-neighborhood of p, there are no MA points other than those on T_1 and T_2, and no boundary points other than those associated with $\overline{p}$. We will show that with the invalid ordering, an intersection of radial lines occurs inside the ε-neighborhood, yielding an MAT point inside the neighborhood, which is a contradiction.

Consider only one side of the MAT, and suppose that the ordering of points on that side is $q_1\, b_2\, b_1\, q_2$, as shown in Figure 8. Let l_1 and l_2 be the line segments connecting b_1 to p and b_2 to p, respectively. Without loss of generality, assume that $p = (0, 0, r_1)$ and q_1 lies on the x-axis, in the negative direction, as shown on the right in Figure 8. Let β_1 be the angle between l_1 and the horizontal and let β_2 be the angle between l_2 and the horizontal, measured from the positive horizontal direction. Let $\overline{\beta_2} = \pi - \beta_2$ and let $\eta = \beta_2 - \beta_1$.

Now, suppose a point $p_\delta = (-\delta, 0, r_\delta)$ along T_1 is chosen such that

$$\delta < \frac{\sin \eta}{\sin \beta_1} \varepsilon$$

and let l_δ be the radial line emanating from p_δ Then $\triangle p\, p_\delta\, i$ has interior angles β_1, $\overline{\beta_2}$, and η, so

$$||\overline{p\, i}|| = \frac{\sin \beta_1}{\sin \eta} \delta < \varepsilon$$

Also, $||\overline{p_\delta\, i}|| < r_\delta$ since otherwise a boundary point would exist inside the ε-neighborhood about p, a contradiction to our assumption. Thus the two radial lines l_2 and l_δ intersect at a point inside the ε-neighborhood about p. Since this contradicts our assumption, the ordering of points must be invalid. $\square$

There are several important implications of this result. First, it shows that one boundary point from each tangent must lie on each side of the MAT, and it indicates the necessary order. It also shows that if the MA is smooth but a discontinuity occurs in the r-component of the MAT, then finite contact must exist on both boundaries related to p. Further, if the MA has a discontinuous tangent at p, then the radial component of the MAT must also have a tangent discontinuity, and finite contact must occur on at least one side. Finally, it demonstrates that the MAT cannot be concave down in the r-direction at a tangent discontinuous point, since then a crossing of the radial lines would necessarily occur on at least one side of the MAT.

5 An Error Bound

Suppose one is given a boundary B which has MAT M. If a computational method is used to generate M, the result is actually some perturbed MAT $\tilde{M}$. For a point on M, the technique presented in Section 3 will produce the exact related boundary points b_1 and b_2 on B. However, if instead a point on $\tilde{M}$ is used, the computed boundary points will contain error propogated from the error in the medial axis computation and points $\tilde{b}_1$ and $\tilde{b}_2$ will be obtained instead of b_1 and b_2. In this section we give a bound for the error between the computed and the actual boundary points.

The error can be divided into two components, one linear and one radial. Referring to Figure 9, the linear component l_1 stems from the distance between the actual MA point $p = (x, y)$ and the computed point $\tilde{p} = (\tilde{x}, \tilde{y})$. The radial component arises from the difference in the directions of the radial lines emanating from the MA point. If the points p and $\tilde{p}$ are identical but the tangents $T = (x', y', r')$ and $\tilde{T} = (\tilde{x}', \tilde{y}', \tilde{r}')$ differ, then the angles α and $\tilde{\alpha}$ will differ. Further, since in the boundary point computation this angle is measured in the xy-plane relative to the projection of the tangent from which it was computed, the angle between the two tangents also contributes to the radial component of the error. Final contributions to the radial component come from the maximum size of r and $\tilde{r}$ and the relative difference in r and $\tilde{r}$. The size is a factor since the distance between two points on opposite rays comprising an angle increases as the points move further out

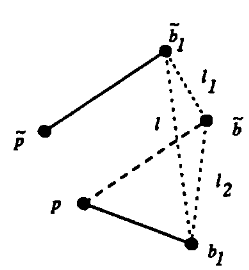

FIGURE 9: Error between actual and computed boundary points.

along the rays. In Figure 9 the radial component is shown as the distance l_2 between b_1 and $\tilde{b}$, where $\tilde{b}$ is the location of $\tilde{b}_1$ without the linear translation due to differences in p and $\tilde{p}$.

In this analysis we will focus on only one boundary point b_1 on an arbitrary side of T, and the corresponding boundary point $\tilde{b}_1$ on the same side of $\tilde{T}$. Without loss of generality, we assume that $T = (1, 0, r')$ and that the angle η between T and $\tilde{T}$ in the xy-plane satisfies $0 \leq \eta << \pi/2$, that is, η is a small angle measured counterclockwise from T. Then the angle between the radial line containing b_1 and that containing $\tilde{b}$ is $\eta + |\alpha - \tilde{\alpha}|$, as seen in Figure 10. With this arrangement, we now have the following error measure.

Theorem 5.1 *Using the notation above, and letting $R = max(r, \tilde{r})$, suppose that*

$$||p - \tilde{p}|| < \varepsilon_1 \tag{1}$$

$$\frac{|r - \tilde{r}|}{R} < \varepsilon_2 \tag{2}$$

$$\eta + |\tilde{\alpha} - \alpha| < \varepsilon_3 \tag{3}$$

Then

$$||b_1 - \tilde{b}_1|| < \varepsilon_1 + R\sqrt{\varepsilon_2{}^2 + 2(1 - \cos\varepsilon_3)} \tag{4}$$

Proof:

Figure 9 shows the most extreme possible situation for the distance between b_1 and $\tilde{b}_1$, that is, the case where it is the length of the hypotenuse of the triangle with legs l_1 and l_2. By the triangle inequality,

$$||b_1 - \tilde{b}_1|| = l \leq l_1 + l_2 \tag{5}$$

By (1),

$$l_1 < \varepsilon_1 \tag{6}$$

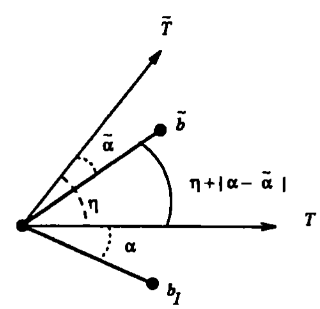

FIGURE 10: Angle relationship

From the Law of Cosines,

$$\begin{aligned} l_2 &= \sqrt{r^2 + \tilde{r}^2 - 2\cos(\eta + |\tilde{\alpha} - \alpha|)} \\ &= \sqrt{(r - \tilde{r})^2 + 2r\tilde{r}(1 - \cos(\eta + |\tilde{\alpha} - \alpha|))} \end{aligned}$$

Without loss of generality, suppose that $r \geq \tilde{r}$. Then

$$\begin{aligned} l_2 &\leq \sqrt{(r - \tilde{r})^2 + 2r^2(1 - \cos(\eta + |\tilde{\alpha} - \alpha|))} \\ &= r\sqrt{(\frac{r - \tilde{r}}{r})^2 + 2(1 - \cos(\eta + |\tilde{\alpha} - \alpha|))} \end{aligned}$$

By (2),

$$(\frac{r - \tilde{r}}{r})^2 < {\varepsilon_2}^2$$

and from (3),

$$\cos(\eta + |\tilde{\alpha} - \alpha|) > \cos\varepsilon_3$$

so that

$$1 - \cos(\eta + |\tilde{\alpha} - \alpha|) < 1 - \cos\varepsilon_3$$

Hence

$$l_2 < R\sqrt{{\varepsilon_2}^2 + 2(1 - \cos\varepsilon_3)} \tag{7}$$

Combining (5) with (6) and (7), we arrive at the asserted relationship (4). □

This relationship makes clear the three separate components of the error, specifically, the difference in location of the MA points in the plane, the relative difference in distance to the boundary, and the angular difference in the radial lines. Although two of these are subsumed in the radial component, the entire expression approaches zero if and only if all three of these differences approach zero independently.

6 Algorithm and Results

Applying the theory of the previous sections, we have implemented an algorithm which given an MAT generates the related boundary. The algorithm assumes that the MAT M is a connected set of line segments, given as sequences of vertices, but allows the MAT to have loops. The input can either be read from a file or input graphically. With either type of input, the output is an ordered set of two-dimensional points and circular arcs which when connected in order approximate the boundary related to M. The output is automatically displayed in the output window unless an invalid MAT has been entered. Optionally, the output can be sent to a file. The user-interface allows graphical modification of the MAT which results in immediate update of the boundary, or an indication that the change has caused the MAT to become invalid. The user can also interactively add, delete, or subdivide edges at any time. These features make it possible to obtain a better understanding of the relationship between changes in the radius function and the resulting changes in the boundary. Figure 11 shows an example of the program in operation, where the bottom right is the output window, and the other three windows are planar input windows. The top left window is the XY-input plane, and contains the MA of the object.

The first step of the boundary generation involves computing the angle between an edge and the radial lines connecting any point on the edge to its related boundary points. Since we are dealing with line segments, this angle is the same for all points on the edge, and can be computed by

$$\alpha_i = \arccos \frac{|r_1 - r_2|}{\sqrt{(x_1 - x_2)^2 + (y_1 - y_2)^2}}$$

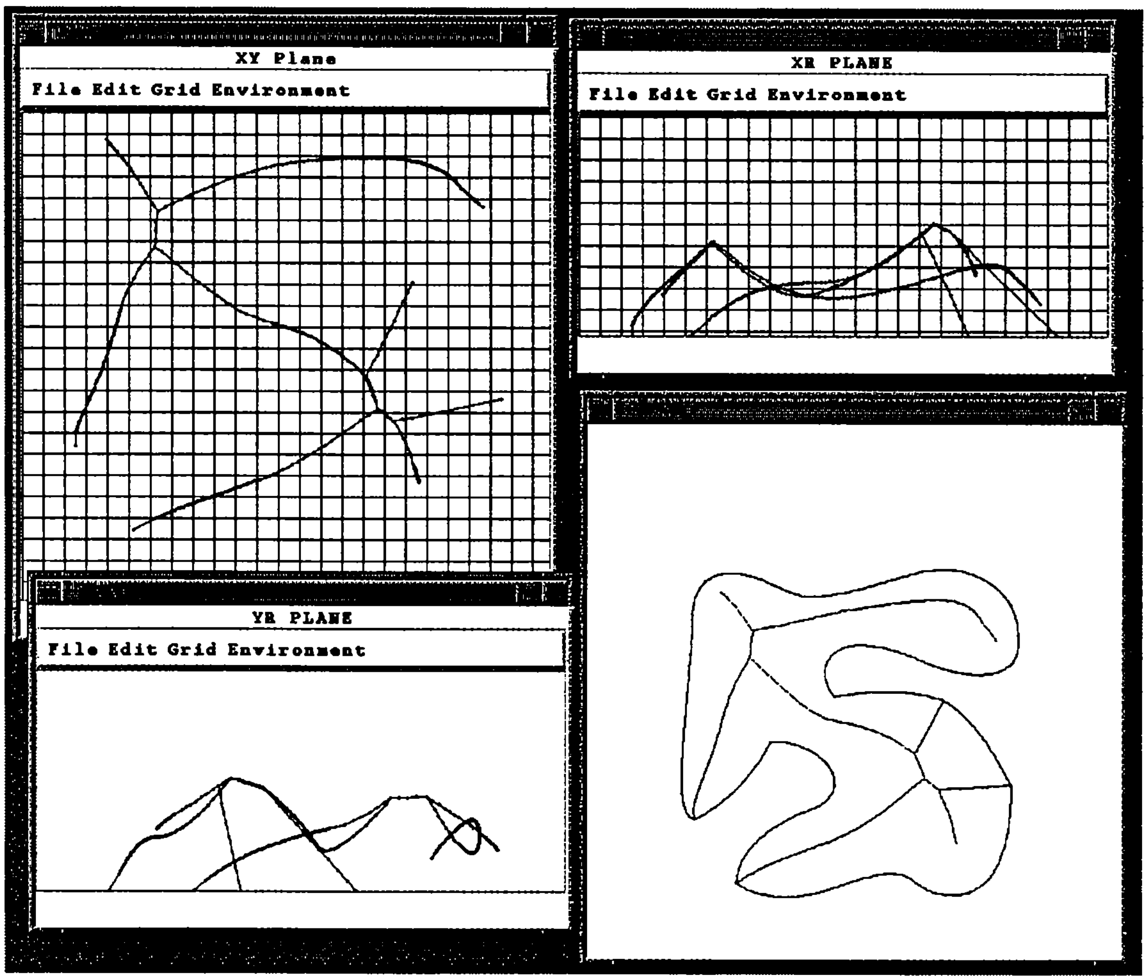

FIGURE 11: User-interface for MAT conversion program

where $v_1 = (x_1, y_1, r_1)$ and $v_2 = (x_2, y_2, r_2)$ are the vertices delimiting edge e_i. This incurs the restriction $0 \leq \alpha_i \leq \pi/2$, which must be taken into account when the rotation to find the boundary points is done. To simplify later computation, the angle is adjusted by the angle the edge makes with the x-direction. Thus at the completion of this step of the algorithm, each edge has two angles associated with it, $\alpha_{i,1}$ and $\alpha_{i,2}$.

The second step is a depth first walk of M to generate the boundary elements related to the vertices. Each vertex has associated with it the same number of boundary elements as it has adjacent edges. The boundary elements related to a particular vertex are not all computed at the same time, however. Instead, each time a vertex is passed in the search, a single boundary element is computed. The element computed at any specific traversal past a vertex is the one which continues the current boundary loop, or the beginning of a new boundary loop if there is no current loop. At the end of this step, there are k boundary loops, one for each loop in the MAT.

The type of boundary element to produce is determined by the angles between adjacent edges of a vertex. For end points, there is only one adjacent edge, so its edge angles determine whether the boundary element is a single point or a circular arc. For normal points and branch points, two edges are involved in the computation of each boundary element. If these two edges are nearly the same, the MAT is assumed to be smooth, and the angles associated with the two edges are averaged to generate a single point. Otherwise, the order of the two boundary points, generated by the two edge angles separately, is checked for validity, and if it is valid, a circular arc delimited by these two points is computed as the boundary element for the vertex.

Figures 12 and 13 show example computations with our algorithm. Figures 12 shows two boundaries, and on the following page, Figure 13 shows the projection of the MATs computed from these objects, along with the new boundaries computed from those MATs. The MAT for the top figure was computed by hand, while that for the bottom object was computed using Chiang's two-dimensional MAT computation program [Chi92]. By lining up the two pages and holding them up to a light, the accuracy of the reconstruction from the MAT can be judged.

7 Conclusions and Future Work

For the two-dimensional problem, the straightforward case-by-case analysis of MAT points presented here allows a conversion from the MAT to a boundary representation of an object. The accuracy of the conversion depends only on the accuracy of the input MAT and the error induced from approximating smooth curves with line segments.

Currently, we are working to extend the conversion theory to three-dimensional objects. Here the classification of MAT points becomes more challenging, since now the MAT is composed of surface patches, some possibly degenerate, in four-space. However, the basic theory of Section 3.1 extends naturally, from which the subsequent theory should also be attainable.

Acknowledgements

Support for this work has been provided by the AT&T Foundation, and by the National Science Foundation under Grant CDR 8803017 to the Engineering Research Center for Intelligent Manufacturing Systems.

The insights of and discussions with my advisor Chris Hoffmann and with Ching-Shoei Chiang and George Vaněček have also contributed to this work.

References

[Blu64] Harry Blum. A transformation for extracting new descriptors of shape. In *Symposium on Models for the Perception of Speech and Visual Form*, pages 362–380. M. I. T. Press, 1964.

[Blu73] Harry Blum. Biological shape and visual science (Part I). *J. Theor. Biol.*, 38:205–287, 1973.

[BN78] Harry Blum and Roger N. Nagel. Shape description using weighted symmetric axis features. *Pattern Recognition*, 10:167–180, 1978.

[Chi92] Ching-Shoei Chiang. *The Euclidean Distance Transform.* PhD thesis, Purdue University, 1992.

[DH73] Richard O. Duda and Peter E. Hart. *Pattern Classification and Scene Analysis.* John Wiley & Sons, 1973.

[Gur89] H. N. Gursoy. *Shape Interrogation by Medial Axis Transform for Automated Analysis.* PhD thesis, M. I. T., 1989.

[Hof92] Christoph M. Hoffmann. Computer vision, descriptive geometry, and classical mechanics. In *Computer Graphics and Mathematics.* Springer-Verlag, 1992.

[HV92] Christoph M. Hoffmann and George Vaněček, Jr. Fundamental techniques for geometric and solid modeling. In C. T. Leondes, editor, *Advances in Control and Dynamics.* Academic Press, 1992.

[MK29] E. Muller and J. Krames. *Die Zyklographie.* Franz Deuticke, Leipzig und Wien, 1929.

[PG90] N. M. Patrikalakis and H. N. Gursoy. Shape interrogation by medial axis transform. Technical Report 90-2, M. I. T. Design Laboratory, 1990.

[Wol92] F.E. Wolter. Cut locus and medial axis in global shape interrogation and representation. Technical Report 92-2, MIT Dept. of Ocean Engineering, 1992.

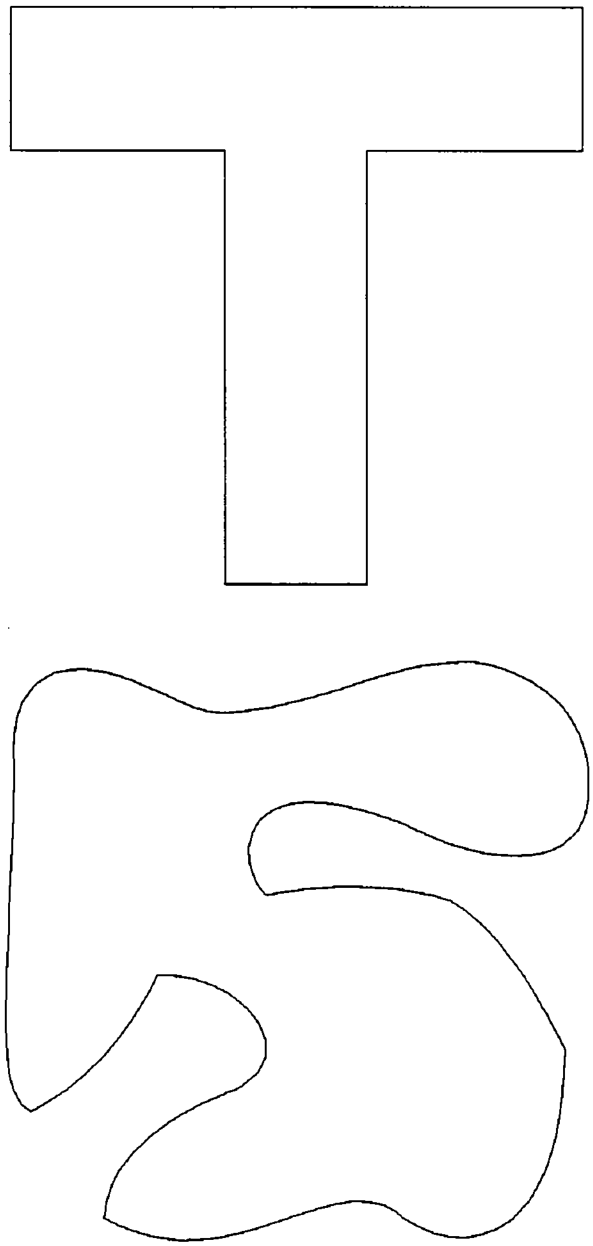

FIGURE 12: Original boundaries

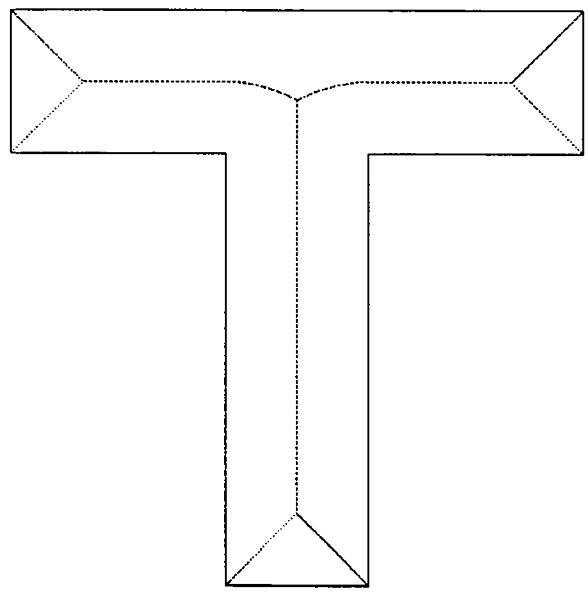

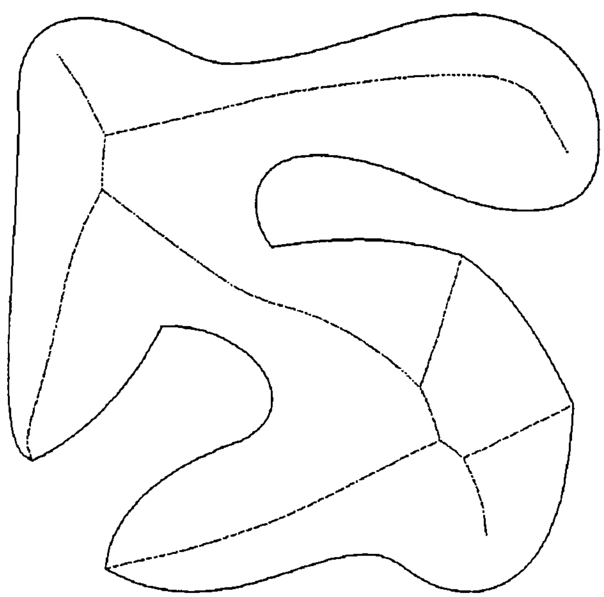

FIGURE 13: The MAs and boundaries computed from them